

# Dynamics of gelling liquids: a short survey

Henning Löwe, Peter Müller and Annette Zippelius

Institut für Theoretische Physik, Georg-August-Universität, D-37077 Göttingen, Germany

Version of 21 December 2004

*Dedicated to Lothar Schäfer on the occasion of his 60<sup>th</sup> birthday*

**Abstract.** The dynamics of randomly crosslinked liquids is addressed via a Rouse- and a Zimm-type model with crosslink statistics taken either from bond percolation or Erdős–Rényi random graphs. While the Rouse-type model isolates the effects of the random connectivity on the dynamics of molecular clusters, the Zimm-type model also accounts for hydrodynamic interactions on a preaveraged level. The incoherent intermediate scattering function is computed in thermal equilibrium, its critical behaviour near the sol-gel transition is analysed and related to the scaling of cluster diffusion constants at the critical point. Second, non-equilibrium dynamics is studied by looking at stress relaxation in a simple shear flow. Anomalous stress relaxation and critical rheological properties are derived. Some of the results contradict long-standing scaling arguments, which are shown to be flawed by inconsistencies.

## 1. Introduction

Gelling liquids are part of everyday life. One encounters them, for example, when preparing a chocolate pudding or when sticking two materials together with the help of glue. From a microscopic point of view, gelling liquids consist of irregularly structured clusters of molecules or macromolecules. The formation of these clusters is either a result of intermolecular association, produced by e.g. van der Waals forces, electrostatic attractions or hydrogen bonding, or a result of chemical reactions such as polycondensation, polymerisation or vulcanisation induced by a chemical crosslinker [1, 2]. Intermolecular association, also called physical gelation, leads to weakly bound clusters, which typically form and dissolve reversibly in the course of time during an experiment. On the other hand, chemical gelation leads to permanent clusters at temperatures of interest, and it is this situation that we will exclusively consider here.

When increasing the concentration of crosslinks in a liquid (sol) one observes a more and more viscous behaviour under shear stresses, until a sudden transformation to an amorphous solid state takes place at a certain critical crosslink concentration. This point marks the gelation transition or sol-gel transition. The static shear viscosity diverges at the transition, and the onset of a static shear modulus is found.

Carothers [3] was the first to interpret the gelation transition as due to the formation of a macroscopic cluster of molecules in the system. His considerations were quantified and refined by Flory [4, 5] and Stockmayer [6, 7] to what is nowadays called “classical theory”, a percolation model of tree-like structures, closely related to percolation on Bethe lattices [8]. So the classical theory arises [9] in the mean-field approximation of lattice-bond percolation [10]. Stauffer [11] and de Gennes [12] suggested the latter as a mathematical model for gelation, in particular, if caused by polycondensation. Lattice-bond-percolation clusters may also contain loops, and the spatial dimension becomes relevant, too. More importantly, upon identifying the gelation transition with the lattice-bond-percolation transition, it is revealed to be a continuous phase transition. Its driving parameter is crosslink concentration, not temperature. Within this theoretical picture, the critical behaviour at the gelation transition is dictated by scaling and universality [13, 10].

The resulting predictions for static properties of gelation clusters agree well with experiments in the vicinity of the sol-gel transition [14, 15]—a substantial improvement over the mean-field like classical theory. As far as dynamical phenomena are concerned, a variety of competing attempts have been made to seek an interpretation in terms of the percolation picture, see e.g. [16–18] for contradictory predictions concerning the shear viscosity. Yet, all of these attempts rely on more or less *ad hoc* assumptions needed to compensate for the lack of thermal fluctuations or any sort of dynamics in a pure percolation model. Rather, the appropriate strategy should be to start from a (semi-) microscopic dynamical model for gelation clusters, from which the desired link to quantities in percolation theory can be *deduced*. This route will be followed here. Other analytical approaches to gelation from a microscopic model include [19–27]. Among others, they describe thermostatic fluctuations in the gel phase and calculate the static shear modulus. Computer simulations of microscopic models for gelation have been done by e.g. [28–34].

In this survey we will concentrate on the sol phase and report on results obtained in [35–42]. The dynamics of the sol phase is characterised by strong precursors of the gelation transition, even well below it. These include anomalous, stretched-exponential decays in time of both dynamical density correlations [43] and shear-stress relaxation [44]. Both decays are characterised by typical time scales which diverge when the critical crosslink concentration is approached. Our exact results on critical rheological properties contradict long-standing scaling arguments, which are shown to be flawed by inconsistencies.

The paper is organised as follows. In Section 2 we briefly lay out a suitable generalisation of the usual Rouse and Zimm model for linear polymers to describe gelling liquids. The model is then used to investigate time-dependent density fluctuations in Section 3. Section 4 deals with stress relaxation and critical rheological properties in a simple shear flow. Both Section 3 and Section 4 are subdivided in a part pertaining to the Rouse model, a part pertaining to the Zimm model and a part where the results are discussed and put in a wider perspective. Finally, Section 5 adds some closing remarks.

## 2. Rouse and Zimm model for randomly crosslinked monomers

In this section we give a brief description of a model which is to be considered a theoretical minimal model for the dynamics of gelling complex fluids. This model is a generalisation of one of the most fundamental models of polymer physics [45–48] to the case of randomly connected monomers. In this context, it has been discussed before by e.g. [49–56, 35, 37–39, 57–59, 40–42].

### 2.1. Dynamical equation

We consider  $N$  point-like monomers, which are characterised by their time-dependent position vectors  $\mathbf{R}_i(t)$ ,  $i = 1, \dots, N$ , in three-dimensional Euclidean space  $\mathbb{R}^3$ . Permanently formed, harmonic crosslinks connect  $M$  randomly chosen pairs of particles  $(i_e, j_e)$ , where  $1 \leq i_e \neq j_e \leq N$  for all  $e = 1, \dots, M$ . The potential energy associated with these entropic Hookean springs takes the form

$$V := \frac{3}{2a^2} \sum_{e=1}^M (\mathbf{R}_{i_e} - \mathbf{R}_{j_e})^2 =: \frac{3}{2a^2} \sum_{i,j=1}^N \mathbf{R}_i \cdot \Gamma_{i,j} \mathbf{R}_j, \quad (1)$$

where the length  $a > 0$  plays the role of an inverse crosslink strength, and physical units have been chosen such that  $k_B T = 1$ . It will be convenient to specify a given crosslink configuration  $\mathcal{G} := \{(i_e, j_e)\}_{e=1}^M$  in terms of its  $N \times N$ -connectivity matrix  $\Gamma$ , which is defined by the right equality in (1). For part of what follows this setting could be generalised to the crosslinking of  $N$  identical molecular units which consist themselves of a given number of monomers that are connected in some fixed manner, such as  $N$  identical chains, rings or stars of monomers [37, 38]. For the ease of presentation, however, we will not consider such a generalisation here.

We study the dynamics of these harmonically crosslinked monomers in the presence of an incompressible solvent fluid, which may induce hydrodynamic interactions between them. Hydrodynamic interactions will be incorporated on a preaveraged level in the spirit of Kirkwood and Riseman [60] and Zimm [46]. This is a traditionally accepted way of doing so albeit the limitations of this approach are still not sufficiently well explored [47, 48]. We also allow for the presence of an externally imposed, simple shear flow in  $x$ -direction

$$\mathbf{v}(\mathbf{r}, t) := \dot{\gamma}(t) y \mathbf{e}_x \quad (2)$$

with a time-dependent shear rate  $\dot{\gamma}(t)$ . Here  $\mathbf{r} = (x, y, z)$ . A purely relaxational monomer dynamics is then described by [47, 48]

$$\frac{d}{dt} \mathbf{R}_i(t) - \mathbf{v}(\mathbf{R}_i(t), t) = - \sum_{j=1}^N \mathbf{H}_{i,j}^{\text{eq}} \frac{\partial V}{\partial \mathbf{R}_j(t)} + \boldsymbol{\xi}_i(t) \quad (3)$$

for  $i = 1, \dots, n$ . This is the defining equation of the *Zimm model for crosslinked monomers (in solution)*. The rest of this subsection is devoted to a brief explanation and discussion of (3), see [41, 42] for more details.

The jointly Gaussian thermal noises  $\boldsymbol{\xi}_i$  in (3) have zero mean and covariance  $\overline{\boldsymbol{\xi}_i(t) \boldsymbol{\xi}_j^\dagger(t')} = 2 \mathbf{H}_{i,j}^{\text{eq}} \delta(t - t') \mathbf{1}$ , as is required by the fluctuation-response theorem. As usual, the  $\boldsymbol{\xi}_i$  “thermalize” the system in the long-time limit. Here, the dagger denotes the transposition of a vector,  $\delta$  the Dirac-delta function and  $\mathbf{1}$  the  $3 \times 3$ -unit matrix.

Interactions between the monomers and the solvent fluid are subsumed in the spatially isotropic and homogeneous preaveraged mobility matrix

$$\mathbf{H}_{i,j}^{\text{eq}} := \frac{1}{\zeta} \left[ \delta_{i,j} + (1 - \delta_{i,j}) h(\kappa^2 \pi / \mathcal{R}_{i,j}) \right]. \quad (4)$$

It emerges [41, 42] from taking Oseen’s expression [61, 60] for the mobility tensor and averaging it with respect to the suitably normalised Boltzmann weight  $\sim e^{-V}$ . However, when it is indispensable to have a positive definite mobility matrix in the sequel, we will replace the Oseen tensor with the Rotne–Prager–Yamakawa tensor [62, 63] in this procedure. Depending on which tensor is used, the function  $h$  in (4) is given by [64]

$$h(x) := \begin{cases} \sqrt{x/\pi} & \text{Oseen,} \\ \text{erf}(\sqrt{x}) - (1 - e^{-x})/\sqrt{\pi x} & \text{Rotne–Prager–Yamakawa.} \end{cases} \quad (5)$$

The expression in the second line of (5) involves the error function  $\text{erf}$  and reduces to the expression of the Oseen case asymptotically as  $x \downarrow 0$ . The diagonal term in the preaveraged mobility matrix (4), which is proportional to the Kronecker symbol  $\delta_{i,j}$ , accounts for a frictional force with friction constant  $\zeta$  that acts when a monomer moves relative to the externally imposed flow field (2). The non-diagonal term reflects the solvent-mediated average influence of the motion of monomer  $j$  on monomer  $i$ . The parameter  $\kappa := \sqrt{6/\pi} \zeta / (6\pi\eta_s a)$  involves the solvent viscosity  $\eta_s$  and serves as the coupling constant of the hydrodynamic interaction. Formally setting  $\kappa = 0$  in (4) yields  $H_{i,j}^{\text{eq}} = \zeta^{-1} \delta_{i,j}$ , and the Zimm model for crosslinked monomers reduces to the *Rouse model for crosslinked monomers* [35–40]

$$\frac{d}{dt} \mathbf{R}_i(t) - \mathbf{v}(\mathbf{R}_i(t), t) = -\frac{1}{\zeta} \frac{\partial V}{\partial \mathbf{R}_i(t)} + \boldsymbol{\xi}_i(t), \quad (6)$$

where  $i = 1, \dots, n$  and the jointly Gaussian thermal noises  $\boldsymbol{\xi}_i$  have zero mean and covariance  $\overline{\boldsymbol{\xi}_i(t) \boldsymbol{\xi}_j^\dagger(t')} = (2/\zeta) \delta(t - t') \mathbf{1}$ . It is only for convenience that we introduced the Rouse model as the special case  $\kappa = 0$  of the Zimm model here. Physically, it has its own standing as *the* minimal model for polymer melts under theta conditions, see e.g. [47, 48] for the case of linear polymer chains. In particular, all the approximations that entered the derivation of the (off-diagonal part of the) preaveraged mobility matrix  $H^{\text{eq}}$  do not affect the Rouse model, of course.

It remains to explain the quantity  $\mathcal{R}_{i,j}$  in (4), which is simply the mean squared displacement between monomers  $i$  and  $j$  in the thermal-equilibrium state characterised by the suitably normalised Boltzmann weight  $\sim e^{-V}$ . In order to write down a formula for  $\mathcal{R}_{i,j}$ , let us remark that, by construction, the connectivity matrix  $\Gamma \equiv \Gamma(\mathcal{G})$  is block-diagonal with respect to the clusters of a given crosslink configuration  $\mathcal{G}$  (which are the maximal connected components of  $\mathcal{G}$ ). Moreover,  $\Gamma(\mathcal{G})$  possesses as many zero eigenvalues as there are clusters in  $\mathcal{G}$ . This is easily seen from the fact that the centre of mass of each cluster does not feel a force from the potential energy  $V$ . Hence,  $\Gamma$  cannot be inverted, but it possesses a Moore–Penrose pseudo-inverse  $Z$  [65], which is the inverse of  $\Gamma$  on the complement of its zero eigenspace and zero elsewhere. It can be represented as  $Z := (1 - E_0)/\Gamma$ , where  $E_0$  denotes the projector on the zero eigenspace of  $\Gamma$  in  $\mathbb{R}^N$  and  $1$  denotes the  $N \times N$ -unit matrix. The mean-squared displacement  $\mathcal{R}_{i,j}$  is then given in terms of  $Z$  according to

$$\mathcal{R}_{i,j} := \begin{cases} Z_{i,i} + Z_{j,j} - 2Z_{i,j} & \text{if } i \text{ and } j \text{ belong to the same cluster,} \\ +\infty & \text{otherwise.} \end{cases} \quad (7)$$

There is also another interpretation for  $\mathcal{R}_{i,j}$ , which we will use below: Viewing each monomer as an electric contact and each crosslink as a unit Ohmian resistor connecting two contacts,  $\mathcal{R}_{i,j}$  is the effective electric resistance between the contacts  $i$  and  $j$  of this corresponding electrical resistor network [66]. This *exact* correspondence between Hookean bead-spring clusters and Ohmian electrical resistor networks relies on the linearity of Hooke’s and Ohm’s law.

Since both the connectivity matrix  $\Gamma$  and the preaveraged mobility matrix  $H^{\text{eq}}$  are block-diagonal, it follows that clusters move *independently* of each other in this model. The salient feature of the Zimm and Rouse equations (3) and (6) is that they are linear in the monomers’ positions. Hence, they admit an explicitly known solution. The results we present in this paper rely heavily on this solution.

## 2.2. Average over crosslink ensemble

So far, everything in this section was meant for an arbitrary but fixed realisation  $\mathcal{G}$  of  $M$  crosslinks among  $N$  monomers. For practical reasons,  $\mathcal{G}$  can never be determined experimentally in macroscopically large gelling fluids. Neither should physically meaningful observables depend on specific microscopic details of  $\mathcal{G}$ , but only on some macroscopic characteristics of it. Therefore, we follow the general philosophy of the theory of disordered systems and take  $\mathcal{G}$  as an element of a statistical ensemble of crosslink configurations, within which it occurs with probability  $P_N(\mathcal{G})$ . The just made statement on physically meaningful observables  $A(\mathcal{G})$  now translates into a *self-averaging property*: the two quantities  $A(\mathcal{G})$  and its ensemble average  $\sum_{\mathcal{G}'} P_N(\mathcal{G}') A(\mathcal{G}')$  coincide (with probability one) in the macroscopic limit. Therefore we will compute the macroscopic limit

$$\langle A \rangle := \lim_{N \rightarrow \infty} \sum_{\mathcal{G}} P_N(\mathcal{G}) A(\mathcal{G}) \quad (8)$$

of such averages with a fixed *crosslink concentration*  $c := \lim_{N \rightarrow \infty} M/N$ . This will be done for two different crosslink ensembles.

(i) Clusters are generated according to three-dimensional continuum percolation, which is closely related to the intuitive picture of gelation, where monomers are more likely to be crosslinked when they are close to each other. Since continuum percolation and lattice percolation are believed to be in the same universality class [10], we employ the scaling description of the latter. It predicts [10] a cluster-size distribution of the form

$$\tau_n \sim n^{-\tau} \exp\{-n/n^*\} \quad (9)$$

for  $\varepsilon := (c_{\text{crit}} - c) \ll 1$  and  $n \rightarrow \infty$  with a typical cluster size  $n^*(\varepsilon) \sim \varepsilon^{-1/\sigma}$  that diverges as  $\varepsilon \rightarrow 0$ . Here,  $\sigma$  and  $\tau$  are (static) critical exponents, see Table 1 below for their numerical values.

(ii) Each pair of monomers is chosen independently with equal probability  $c/N$ , corresponding to Erdős–Rényi random graphs, which are known to resemble the critical properties of mean-field percolation [9]. After performing the macroscopic limit, there is no macroscopic cluster for  $c < c_{\text{crit}} = 1/2$  and almost all clusters are trees [67]. Furthermore, all  $n^{n-2}$  trees of a given “size”  $n$ , that is, with  $n$  monomers, are equally likely. The cluster-size distribution can also be cast into the scaling form (9) with the exactly known critical exponents  $\tau$  and  $\sigma$  listed below in Table 1.

## 3. Time-dependent density fluctuations

In this section we address dynamical properties of gelling liquids in thermal equilibrium. Therefore we will assume throughout this section that there is no externally imposed shear flow, i.e.  $\dot{\gamma} = 0$ .

Experiments [43, 68] on quasi-elastic light scattering in gelling liquids allow to measure how spatial density fluctuations of a given wave vector  $\mathbf{q}$  are correlated to each other at different times  $t$ . This information is encoded in the incoherent intermediate scattering function

$$S(\mathbf{q}, t) := \lim_{t_0 \rightarrow -\infty} \frac{1}{N} \overline{\sum_{i=1}^N e^{i\mathbf{q} \cdot [\mathbf{R}_i(t+t_0) - \mathbf{R}_i(t_0)]}}. \quad (10)$$

The right-hand side of (10) is determined by the solution  $\mathbf{R}_i(t)$  of the dynamical equation (3) for a given crosslink realisation  $\mathcal{G}$  and with initial conditions being imposed at time  $t_0$ . The

average over the thermal noise and the subsequent limit  $t_0 \rightarrow -\infty$  in (10) ensure that the system reaches its thermal-equilibrium state. Then, for large retardation times  $t$ , one expects [69, 43] that this correlation is determined by the slowest relaxation processes in the system. Due to the independent motion of different clusters in the model under consideration, the slowest relaxation processes correspond to the centre-of-mass diffusion of whole clusters of monomers. This argument can be quantified—see e.g. [35], [41] or Eq. (4.12) in [37]—and yields

$$S(\mathbf{q}, t) \stackrel{t \rightarrow \infty}{\sim} \sum_{k=1}^K \frac{N_k}{N} \exp\{-q^2 t D(\mathcal{N}_k)\}. \quad (11)$$

Here we have set  $q := |\mathbf{q}|$  and introduced the clusters  $\mathcal{N}_k, k = 1, \dots, K$ , of the given crosslink configuration  $\mathcal{G}$ . The number of monomers in the cluster  $\mathcal{N}_k$  is denoted by  $N_k$  and

$$D(\mathcal{N}_k) := \lim_{t \rightarrow \infty} \frac{1}{6t} \overline{[\mathbf{R}_{\text{CM}_k}(t) - \mathbf{R}_{\text{CM}_k}(0)]^2} = \left( \sum_{i,j \in \mathcal{N}_k} \left[ \frac{1}{\mathbf{H}^{\text{eq}}} \right]_{i,j} \right)^{-1} \quad (12)$$

defines its diffusion constant in terms of the mean-square displacement of its centre of mass  $\mathbf{R}_{\text{CM}_k}(t) := N_k^{-1} \sum_{i \in \mathcal{N}_k} \mathbf{R}_i(t)$ . The right equality in (12) follows from a short calculation with the exact solution of the dynamical equation (3). It was previously established in [70]. Another diffusion constant has been introduced by Kirkwood [48, 47]

$$\widehat{D}(\mathcal{N}_k) := \frac{1}{N_k^2} \sum_{i,j \in \mathcal{N}_k} \mathbf{H}_{i,j}^{\text{eq}}. \quad (13)$$

It provides an upper bound to the former,

$$D(\mathcal{N}_k) \leq \widehat{D}(\mathcal{N}_k), \quad (14)$$

as can be shown by applying the Jensen–Peierls inequality, see e.g. Sect. 8c in [71], to (12). Customarily, one also defines an effective diffusion constant  $D_{\text{eff}}$  for the whole gelling liquid by

$$D_{\text{eff}}^{-1} := \lim_{q \rightarrow 0} q^2 \int_0^\infty dt S(\mathbf{q}, t) = \sum_{k=1}^K \frac{N_k}{N} \frac{1}{D(\mathcal{N}_k)}. \quad (15)$$

Since  $S(\mathbf{q}, t)$  is expected to develop a time-persistent part in the gel phase,  $D_{\text{eff}}$  is expected to vanish when approaching the gelation transition from the sol side.

### 3.1. Rouse dynamics

We recall from Sect. 2.1 that in the absence of hydrodynamic interactions,  $\kappa = 0$ , we have  $\mathbf{H}_{i,j}^{\text{eq}} = \zeta^{-1} \delta_{i,j}$ . Hence, the cluster-diffusion constant (12) and the Kirkwood diffusion constant (13) are equal

$$D(\mathcal{N}_k) = \widehat{D}(\mathcal{N}_k) = \frac{1}{\zeta N_k}, \quad (16)$$

and inversely proportional to the number of monomers in the cluster [35]. In other words, cluster topology does not influence diffusion within Rouse dynamics.

Next, we discuss the long-time behaviour of the incoherent intermediate scattering function in the macroscopic limit. According to Sect. 2.2, this amounts to calculating the average of (11)

$$\langle S(\mathbf{q}, t) \rangle \stackrel{t \rightarrow \infty}{\sim} \left\langle \sum_{k=1}^K \frac{N_k}{N} \exp\{-q^2 t D(\mathcal{N}_k)\} \right\rangle. \quad (17)$$

Thanks to (16) this average is easily performed by reordering the clusters according to their size

$$\langle S(\mathbf{q}, t) \rangle \stackrel{t \rightarrow \infty}{\sim} \sum_{n=1}^{\infty} n \tau_n e^{-q^2 t / (\zeta n)}, \quad (18)$$

where

$$\tau_n := \left\langle \sum_{k=1}^K \frac{1}{N} \delta_{N_k, n} \right\rangle \quad (19)$$

is the cluster-size distribution and (18) holds in the absence of an infinite cluster. Using the scaling form (9) of  $\tau_n$ , we find [35, 37]

$$\langle S(\mathbf{q}, t) \rangle \stackrel{t \rightarrow \infty}{\sim} \left( \frac{\zeta}{q^2 t} \right)^y \begin{cases} 1 & \varepsilon = 0, \\ [t/t_q^*(\varepsilon)]^{(y-1/2)/2} \exp\{-\text{const.} [t/t_q^*(\varepsilon)]^{1/2}\} & \varepsilon > 0. \end{cases} \quad (20)$$

At the critical point, the long-time decay is algebraic with a critical exponent  $y = \tau - 2$ . In the sol phase one has a Kohlrausch or stretched-exponential behaviour with a time scale that diverges as  $t_q^*(\varepsilon) \sim (\zeta/q^2) \varepsilon^{-\mu}$  with a critical exponent  $\mu = 1/\sigma$ , when the critical point is approached.

For the effective diffusion constant (15) we conclude from (20) that it vanishes like

$$\langle D_{\text{eff}} \rangle \sim \lim_{q \downarrow 0} [q^2 t_q(\varepsilon)]^{-(3-\tau)} \sim \varepsilon^a \quad \text{with } a = (3 - \tau)/\sigma \quad (21)$$

as  $\varepsilon \downarrow 0$ .

The exponent  $a$  could have also been deduced directly from the right expression in (15). Indeed, given any *cluster-additive observable*, a reordering of the clusters according to their size yields

$$\langle A \rangle = \left\langle \sum_{k=1}^K \frac{N_k}{N} A(\mathcal{N}_k) \right\rangle = \sum_{n=1}^{\infty} n \tau_n \langle A \rangle_n, \quad (22)$$

where

$$\langle A \rangle_n := \frac{1}{\tau_n} \left\langle \sum_{k=1}^K \frac{1}{N} \delta_{N_k, n} A(\mathcal{N}_k) \right\rangle \quad (23)$$

is the partial average of  $A$  over all clusters of a given size  $n$ . Now, if the partial averages exhibit the critical divergence

$$A_n := \langle A \rangle_n \big|_{\varepsilon=0} \sim n^b, \quad (24)$$

then

$$\langle A \rangle \sim \varepsilon^{-u} \quad \text{as } \varepsilon \downarrow 0 \quad \text{with } u = (2 - \tau + b)/\sigma, \quad (25)$$

provided that  $u > 0$ .

**Table 1.** Numerical values for the critical exponents of the cluster-size distribution (9) and the two fractal dimensions of Gaussian phantom clusters in (27). The values are listed for cluster statistics according to three-dimensional bond percolation (3D) and Erdős–Rényi random graphs (ER).

	$\tau$	$\sigma$	$d_s$	$d_f^{(G)}$
3D	2.18	0.45	1.33	3.97
ER	5/2	1/2	4/3	4

### 3.2. Zimm dynamics

In contrast to the free-draining limit described by Rouse dynamics in the last subsection, one expects that with hydrodynamic interactions being present, cluster topology will have an influence on the diffusion constants.

For simplicity, let us start with the Kirkwood diffusion constant. In order to extract a size dependence out of  $\hat{D}$ , we look at the average  $\langle \hat{D} \rangle_n$  over all clusters of a given size  $n$  and study its behaviour as a function of  $n$ . More specifically, we will perform this average precisely at the critical concentration  $c_{\text{crit}}$ , where we expect an algebraic decrease as  $n \rightarrow \infty$  due to the absence of any other length scale at criticality. Indeed, using the Oseen tensor for the hydrodynamic interactions we deduce from (13), (4) and (5) that

$$\hat{D}_n := \langle \hat{D} \rangle_n|_{c=c_{\text{crit}}} = \frac{1}{\zeta n} + \frac{\kappa}{\zeta n^2} \sum_{\substack{i,j=1 \\ i \neq j}}^n \langle \mathcal{R}_{i,j}^{-1/2} \rangle_n|_{c=c_{\text{crit}}} \stackrel{n \rightarrow \infty}{\sim} \frac{1}{\zeta} \left( \frac{1}{n} + \frac{\lambda \kappa}{n^{1/d_f^{(G)}}} \right), \quad (26)$$

where  $\lambda$  is some dimensionless proportionality constant. The asymptotic behaviour of the average over the resistances in (26) is derived in [41]. The derivation has to distinguish between the two different cases for the crosslink ensemble. For Erdős–Rényi random graphs the asymptotics can be deduced from the exact probability distribution of  $\mathcal{R}_{i,j}$  in [72]. For three-dimensional bond percolation we use the scaling form of the probability distribution, which was established within two-loop order of a renormalisation-group treatment of an associated field theory [73, 74]. Equation (26) involves the fractal Hausdorff dimension

$$d_f^{(G)} := 2d_s/(2 - d_s) \quad (27)$$

of Gaussian phantom clusters, which also determines the scaling of their radius of gyration according to [50, 52, 55]

$$R_{\text{gyr},n} := \left[ \frac{1}{2n^2} \sum_{i,j=1}^n \langle (\mathbf{R}_i - \mathbf{R}_j)^2 \rangle_n|_{c=c_{\text{crit}}} \right]^{1/2} \stackrel{n \rightarrow \infty}{\sim} n^{1/d_f^{(G)}}. \quad (28)$$

The other fractal dimension in (27) is the *spectral dimension*  $d_s$  of the incipient percolating cluster [75, 76]. Their numerical values are listed in Table 1. We conclude from (26) that  $\hat{D}_n$  shows a crossover from Rouse behaviour  $\hat{D}_n \sim n^{-1}$  for  $n < \hat{n}(\kappa) \sim \kappa^{-1/(1-1/d_f^{(G)})}$  to Zimm behaviour

$$\hat{D}_n \sim n^{-1/d_f^{(G)}} \sim 1/R_{\text{gyr},n} \quad (29)$$

for asymptotically large  $n > \hat{n}(\kappa)$ .

Now we turn to the averaged diffusion constant

$$D_n := \langle D \rangle_n|_{c=c_{\text{crit}}} \stackrel{n \rightarrow \infty}{\sim} n^{-b_D} \quad (30)$$



of clusters of size  $n$  at the gel point, which is also expected to obey a critical scaling for large cluster sizes  $n$ . From the Jensen-Peierls inequality  $D_n \leq \hat{D}_n$ , see (14), we then infer the inequality

$$b_D \geq 1/d_f^{(G)} \quad (31)$$

for the critical exponents. Figure 1 shows numerical data for the cluster diffusion constant  $D_n$ , plotted against  $n$ , for different values of the hydrodynamic interaction strength  $\kappa$ . The crosslink ensemble in Fig. 1(a) corresponds to Erdős–Rényi random graphs. In Fig. 1(b) crosslinks were chosen according to three-dimensional bond-percolation. In the numerical computations we have used  $H^{\text{eq}}$  corresponding to the Rotne–Prager–Yamakawa tensor so that a positive definite mobility matrix is always guaranteed. Like the Kirkwood diffusion constant,  $D_n$  also exhibits a crossover from Rouse to Zimm behaviour at a cluster size comparable to  $\hat{n}(\kappa)$ . Figure 2 shows the exponent  $b_D$  of the power-law fit (30) to the data of Fig. 1 in the large  $n$ -regime for the different values of  $\kappa$ . The horizontal dashed lines in Figs. 2(a) and (b) correspond to the exponent value  $1/d_f^{(G)}$  of the respective Kirkwood diffusion constant. The bigger exponent values that occur for small values of  $\kappa$  still show residual Rouse behaviour for the largest system sizes we treated. For bigger values of  $\kappa$  the crossover can hardly be felt any more in the largest systems, and the extracted exponent value  $b_D$  corresponds to Zimm dynamics. This value is very close to the scaling exponent in (29) for the Kirkwood diffusion constant, and, in fact, we conjecture that

$$b_D = 1/d_f^{(G)}. \quad (32)$$

We now turn to the long-time behaviour of the incoherent intermediate scattering function (10). The asymptotics (11), (22) and Jensen’s inequality yield the lower bound [41]

$$\langle S(\mathbf{q}, t) \rangle \geq \sum_{n=1}^{\infty} n \tau_n e^{-q^2 t D_n}. \quad (33)$$

In fact, there is numerical evidence that this inequality actually captures the correct long-time asymptotics of  $\langle S(\mathbf{q}, t) \rangle$ . Evaluating the right-hand side of (33) for large times  $t$ , this then leads to the scaling form [41]<sup>‡</sup>

$$\langle S(\mathbf{q}, t) \rangle \stackrel{t \rightarrow \infty}{\sim} \left( \frac{\zeta}{q^2 t} \right)^y \begin{cases} 1 & \varepsilon = 0, \\ [t/t_q^*(\varepsilon)]^{x(y-1/2)} \exp\{-\text{const.} [t/t_q^*(\varepsilon)]^x\} & \varepsilon > 0 \end{cases} \quad (34)$$

with the time scale  $t_q^*(\varepsilon) \stackrel{\varepsilon \downarrow 0}{\sim} q^{-2} \varepsilon^{-z}$ . The exponents are given by

$$x = (1 + b_D)^{-1}, \quad y = (\tau - 2)/b_D, \quad z = b_D/\sigma \quad (35)$$

and are expressed in terms of  $b_D \approx 0.25$ , see (32) and Table 1. The Rouse limit (20) of (34) corresponds to setting  $b_D = 1$  in the above expressions.

The critical vanishing

$$\langle D_{\text{eff}} \rangle \sim \varepsilon^a \quad \text{with} \quad a = (2 - \tau + b_D)/\sigma \quad (36)$$

of the effective diffusion constant follows directly from (22) – (25) provided that  $a > 0$ . This condition is fulfilled for three-dimensional bond percolation where  $a \approx 0.16$ , but violated for Erdős–Rényi random graphs. Finally, we like to point out that, regardless of the cluster statistics, the ensemble averaged diffusion constant  $\langle D \rangle$  never vanishes at the critical point. This is simply because it has non-vanishing contributions from all clusters, which add up.

<sup>‡</sup> Note that there is a misprint in the second line after Eq. (30) in [41]. The algebraic prefactor in the scaling form of the function  $s(\lambda)$  should read  $\lambda^{x(y-1/2)}$  instead of  $\lambda^{xy}$ .

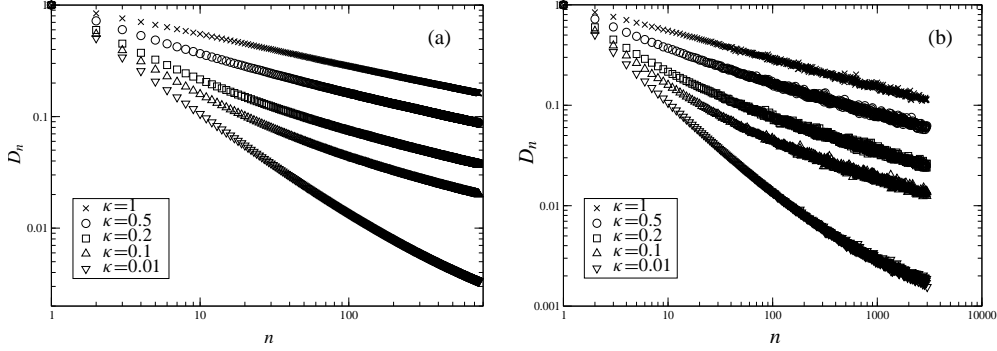


**Figure 1.** (a)  $D_n$  at the gel point for mean field percolation and different hydrodynamic interaction strengths. (b) Same for three-dimensional bond percolation.

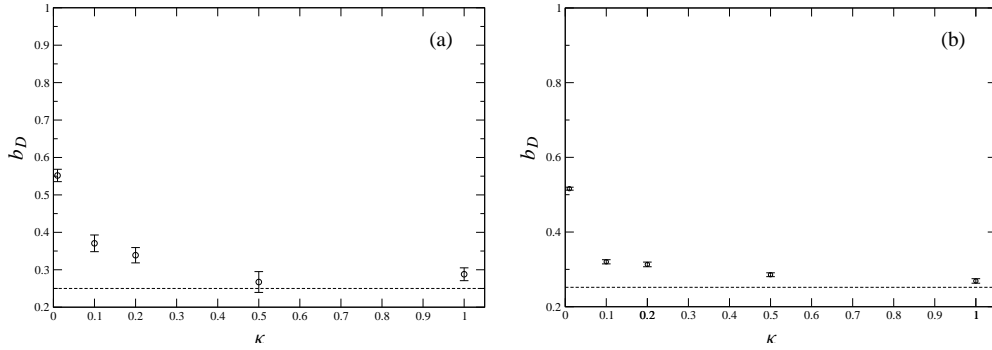


**Figure 2.** (a) Critical exponents  $b_D$ , corresponding to a power-law fit  $D_n \sim n^{-b_D}$  in Fig. 1(a). (b) Same for Fig. 1(b).

### 3.3. Discussion

We have studied the critical scaling  $D_n \sim n^{-b_D}$  of the averaged cluster diffusion constants over clusters of size  $n$  and used it to obtain the scaling behaviour of the intermediate incoherent scattering function  $\langle S(\mathbf{q}, t) \rangle$  near criticality. The associated critical exponents are summarised in Table 2. Within Rouse dynamics cluster diffusion constants are inversely proportional to the cluster size  $n$ , irrespective of the cluster topology, that is,  $b_D = 1$ . Zimm dynamics leads to  $b_D = 1/d_f^{(G)}$ , see (32), and topology does play a role: Indeed, it is well known [48] that within Zimm dynamics the diffusion constant of a *linear chain* of  $n$  monomers decreases as  $n^{-1/2}$ . Since  $b_D \approx 0.25 < 1/2$ , this means that, on average, a monomer in a branched cluster feels less friction—which is intuitively appealing, because monomers in the interior of a cluster should be dragged along. Second, (28), (30) and (32) imply for Zimm dynamics that  $D_n \sim 1/R_{\text{gyr},n}$ . Hence, this relation does not only hold for linear chains, for which it has been well known [48], but in an average sense for *all* percolation clusters.

Concerning the scaling exponents of the incoherent intermediate scattering function, Table 2 shows that neither Rouse nor Zimm dynamics provides even a reasonably good description of the experimental findings, despite their strong scatter. There are several reasons for the discrepancies between the model predictions and experiments. (i) Our results pertain to  $\theta$ -conditions, in so far as excluded-volume interactions have been neglected in the

**Table 2.** Summary of critical exponents for cluster diffusion constants and the incoherent intermediate scattering function (see Eqs. (30), (20) and (34) for their definitions). The numerical values for Rouse and Zimm dynamics—listed for cluster statistics from three-dimensional bond percolation (3D) and Erdős–Rényi random graphs (ER)—are compared to experimental findings.

Exponent	Zimm		Rouse		[68]	[77]	[78]
	3D	ER	3D	ER			
$b_D$	0.25	1/4	1	1			
$x$	0.80	4/5	1/2	1/2	0.66	0.3 – 0.8	0.64
$y$	0.71	2	0.18	1/2	0.27	0.2 – 0.3	0.34
$z$	0.56	1/2	2.22	2	2.5		
$a$	0.16	(*)	1.82	1	1.9	0.5 – 1	1.9

(\*) no divergence

models. Excluded-volume interactions could cause a swelling of the clusters, which results in a different fractal Hausdorff dimension. (ii) We chose cluster statistics according to three-dimensional bond percolation. This accounts well for crosslinking in a dense melt, say, but not in dilute solutions. (iii) It has been suggested [68] that hydrodynamic interactions between monomers in a cluster are screened by smaller clusters in the reaction bath so that the Rouse rather than the Zimm model should apply. Our analysis supports this conclusion in so far as the exponents of the Rouse model are closer to the experimental values. So the more striking failure of the Zimm model can be traced back to a too slow decay of  $D_n$  with  $n$ . (iv) Preaveraging of the hydrodynamic interactions is an uncontrolled approximation, and it remains to be seen what a full treatment of hydrodynamic interactions predicts for the critical dynamics of gelling solutions.

#### 4. Stress relaxation

Gelling liquids exhibit striking rheological properties which have been continuously studied over the years by experiments [79–86], theories [11, 16, 50, 87, 88, 35, 89, 36, 37, 90, 38, 39] and simulations [28, 29, 31, 91, 32–34]. For example, when subjected to the homogeneous shear flow (2), distinct relaxation patterns are observed, which are due to the participation of many different excitation modes of all sorts of clusters. More precisely, experiments suggest the scaling form [92, 44, 80–82, 86, 87]

$$\langle G(t) \rangle \sim t^{-\Delta} g(t/\bar{t}) \quad \text{with} \quad \bar{t}(\varepsilon) \sim \varepsilon^{-\bar{z}} \quad (37)$$

for the macroscopic (shear-) stress-relaxation function in the sol phase for asymptotically long times  $t$  and crosslink concentrations close to the critical point, *i.e.* for  $\varepsilon \ll 1$ . The typical relaxation time  $\bar{t}$  diverges with a critical exponent  $\bar{z} > 0$  for  $\varepsilon \downarrow 0$ . The scaling function  $g$  is of order unity for small arguments so that one finds the algebraic decay  $\langle G(t) \rangle \sim t^{-\Delta}$  with a critical exponent  $0 < \Delta \leq 1$  for  $t \rightarrow \infty$  at the critical point. For large arguments,  $g$  decreases faster than any inverse power. Sometimes a stretched exponential has been proposed for  $g$  in this asymptotic regime [82, 87].

In this section we will investigate to what extent such critical properties can be predicted by the Rouse and the Zimm model. Thus we will explore the consequences of the dynamics (3), resp. (6), in the presence of the externally applied simple shear flow (2). In reaction to the flow, the system of crosslinked monomers builds up an intrinsic shear stress. Following

Kirkwood, see e.g. Chap. 3 in [48] or Chap. 16.3 in [47], this shear stress is given by the force per unit area exerted by the monomers

$$\boldsymbol{\sigma}(t) = \lim_{t_0 \rightarrow -\infty} -\frac{\rho_0}{N} \sum_{i=1}^N \overline{\mathbf{F}_i(t) \mathbf{R}_i^\dagger(t)}. \quad (38)$$

Here,  $\mathbf{R}_i(t)$  is the solution of the equation of motion (3) with some initial condition at time  $t_0$  in the distant past (so that the noise average yields a thermalized state in which all transient effects stemming from the initial condition have died out). Moreover,  $\rho_0$  stands for the monomer concentration and  $\mathbf{F}_i(t) := -\partial V / \partial \mathbf{R}_i(t)$  is the net spring force acting on monomer  $i$  at time  $t$ . The explicit computation [37, 38] of the right-hand side of (38) yields

$$\boldsymbol{\sigma}(t) = G(0) \mathbf{1} + \int_{-\infty}^t dt' G(t-t') \dot{\gamma}(t') \begin{pmatrix} 2 \int_{t'}^t ds \dot{\gamma}(s) & 1 & 0 \\ 1 & 0 & 0 \\ 0 & 0 & 0 \end{pmatrix} \quad (39)$$

for arbitrary strengths of the shear rate  $\dot{\gamma}(t)$ . Here, we have defined the stress-relaxation function

$$G(t) := \frac{\rho_0}{N} \text{Tr} \left[ (1 - \tilde{\mathbf{E}}_0) \exp \left( -\frac{6t}{a^2} \tilde{\Gamma} \right) \right] \quad (40)$$

as a trace over the matrix exponential of  $\tilde{\Gamma} := (\mathbf{H}^{\text{eq}})^{1/2} \Gamma (\mathbf{H}^{\text{eq}})^{1/2}$ . Due to the occurrence of the spectral projector  $\tilde{\mathbf{E}}_0$  on the kernel of  $\tilde{\Gamma}$ , this trace is effectively restricted to the subspace of non-zero eigenvalues.

For a time-independent shear rate  $\dot{\gamma}$ , the shear stress (39) is also independent of time. The viscosity  $\eta$  is then related to shear stress via

$$\eta := \frac{\sigma_{x,y}}{\dot{\gamma} \rho_0} = \frac{1}{\rho_0} \int_0^\infty dt G(t) = \frac{a^2}{3} \frac{1}{2N} \text{Tr} \left[ \frac{1 - \tilde{\mathbf{E}}_0}{\tilde{\Gamma}} \right]. \quad (41)$$

Apparently, the viscosity is determined by the trace of the Moore–Penrose inverse of  $\tilde{\Gamma}$ . The normal stress coefficients are given by

$$\Psi^{(1)} := \frac{\sigma_{x,x} - \sigma_{y,y}}{\dot{\gamma}^2 \rho_0} = \frac{2}{\rho_0} \int_0^\infty dt t G(t) = \left( \frac{a^2}{3} \right)^2 \frac{1}{2N} \text{Tr} \left[ \frac{1 - \tilde{\mathbf{E}}_0}{\tilde{\Gamma}^2} \right] \quad (42)$$

and

$$\Psi^{(2)} := \frac{\sigma_{y,y} - \sigma_{z,z}}{\dot{\gamma}^2 \rho_0} = 0. \quad (43)$$

The vanishing of  $\Psi^{(2)}$  is typical for Rouse/Zimm-type models and has been well known for the case of linear polymers [48]. Since  $\tilde{\Gamma}$  is block-diagonal with respect to the clusters, the observables  $G(t)$ ,  $\eta$  and  $\Psi^{(1)}$  are all cluster-additive in the sense of (22).

The scaling form (37) of the macroscopic stress-relaxation function  $\langle G(t) \rangle$  implies that the macroscopic viscosity and first normal stress coefficient exhibit a critical divergence

$$\langle \eta \rangle \sim \varepsilon^{-k} \quad \text{and} \quad \langle \Psi^{(1)} \rangle \sim \varepsilon^{-\ell} \quad (44)$$

at the sol-gel transition as  $\varepsilon \downarrow 0$  with critical exponents given by the scaling relations [44, 39]

$$k = z(1 - \Delta) \quad \text{and} \quad \ell = z(2 - \Delta) = k + z. \quad (45)$$

Thus, it suffices to know any two of the four critical exponents  $\Delta$ ,  $z$ ,  $k$  and  $\ell$ .

#### 4.1. Rouse dynamics

For Rouse dynamics we have  $\tilde{\Gamma} = \Gamma/\zeta$  so that the computation of the stress-relaxation function, the viscosity or the first normal stress coefficient requires the knowledge of spectral properties of the connectivity matrix  $\Gamma$ .

Concerning the macroscopic viscosity  $\langle\eta\rangle$ , there are several ways of calculating the critical exponent  $k$  in (44). The different ways explore connections to problems in different branches of research. Given a cluster  $\mathcal{N}_k$ , the trace of the Moore–Penrose inverse of  $\Gamma(\mathcal{N}_k)$  can be expressed in terms of the resistances (7) according to [36, 37]

$$\eta(\mathcal{N}_k) = \frac{\zeta a^2}{6N_k} \text{Tr} \left[ \frac{1 - \mathbf{E}_0(\mathcal{N}_k)}{\Gamma(\mathcal{N}_k)} \right] = \frac{\zeta a^2}{12N_k^2} \sum_{i,j \in \mathcal{N}_k} \mathcal{R}_{i,j}. \quad (46)$$

We stress that this is an exact relation [66]. It has nothing to do with electrical analogues put forward in scaling arguments [69]. For the case of Erdős–Rényi random graphs there are only tree clusters for  $c < c_{\text{crit}} = 1/2$ . In this special case the resistance  $\mathcal{R}_{i,j}$  reduces to the graph distance of  $i$  and  $j$  in  $\mathcal{N}_k$ , and the right-hand side of (46) is known as the Wiener index  $W(\mathcal{N}_k)$  in graph theory. From a graph-theoretical point of view, the right equality in (46) follows also as an application of the matrix-tree theorem, see e.g. [93], Thm. 5.5. Moreover, the partial averages  $\langle W \rangle$  are exactly known [72], and, using (22), one finds the exact result [36, 37]

$$\langle\eta\rangle = \frac{\zeta a^2}{24c} \left[ \ln \left( \frac{1}{1-2c} \right) - 2c \right]. \quad (47)$$

It can be interpreted as a critical divergence with exponent  $k = 0$ . Alternatively, (47) can also be obtained from a replica approach [37] instead of using graph theory. The replica approach is also capable of providing us with higher inverse moments  $\langle N^{-1} \text{Tr} [(1 - \mathbf{E}_0)/\Gamma^\nu] \rangle$  for not too large positive integers  $\nu$  [90]. Using these results for  $\nu = 2$ , a (somewhat lengthy) exact expression for  $\Psi^{(1)}$  was derived in [39] for crosslink statistics from Erdős–Rényi random graphs. It exhibits the critical behaviour

$$\langle\Psi^{(1)}\rangle \sim \varepsilon^{-\ell} \quad \text{with} \quad \ell = 3. \quad (48)$$

Now we turn to the crosslink ensemble of three-dimensional bond percolation. In order to proceed from (46) in this case, one needs to know the average resistance  $\langle\mathcal{R}_{i,j}\rangle_n$  between two nodes in bond-percolation clusters of size  $n$ . Luckily, random electric resistance networks have been studied extensively, and the asymptotic behaviour

$$\langle\mathcal{R}_{i,j}\rangle_n \sim n^{b_\eta} \quad \text{with} \quad b_\eta := (2/d_s) - 1 \quad (49)$$

can be extracted [36, 37] from highly developed renormalisation-group treatments of an associated field theory [73, 74]. Thus, (46), (22) and (25) lead to the critical behaviour  $\langle\eta\rangle \sim \varepsilon^{-k}$  with

$$k = (1 - \tau + 2/d_s)/\sigma \quad (50)$$

as  $\varepsilon \downarrow 0$ . Of course, this exact scaling behaviour reduces to the Erdős–Rényi result  $k = 0$  from (47), when inserting the appropriate mean-field values for the exponents.

None of the above approaches is able to yield any of the other critical exponents  $\Delta$  and  $z$ —or also  $\ell$  in the case of three-dimensional percolation statistics. Here, a connection to random walks in random environments is helpful. For the time being, let us concentrate on the case of three-dimensional percolation statistics, where the maximum number of bonds emanating from any vertex is limited to  $m = 6$  on the simple cubic lattice. Now, consider a random walker—coined “blind ant” by de Gennes [12]—that moves along a bond from one

site to another in the same cluster at discrete time steps [10, 76, 94, 95]. If the ant happens to visit site  $i$  at time  $s$ , which is connected with  $m_i \leq m$  bonds to other sites, then it will move with equal probability  $1/m$  along any one of the  $m_i$  bonds within the next time step and stay at site  $i$  with probability  $1 - m_i/m$ . By definition of the connectivity matrix  $\Gamma$  of the cluster, one has  $\Gamma_{ii} = m_i$  for its diagonal matrix elements,  $\Gamma_{ij} = -1$  if two different sites  $i \neq j$  are connected by a bond and zero otherwise. Hence, the associated master equation for the ant's sojourn probability  $p_i(s)$  for site  $i$  at time  $s$  reads

$$p_i(s+1) = (1 - \Gamma_{ii}/m)p_i(s) + \sum_{j \neq i} (-\Gamma_{ij}/m)p_j(s), \quad (51)$$

which is equivalent to

$$p_i(s+1) - p_i(s) = -m^{-1} \sum_j \Gamma_{ij} p_j(s). \quad (52)$$

Here the summation extends over all sites in the cluster. For long times  $s \gg 1$ , it is legitimate to replace the difference (quotient) on the left-hand side of (52) by a derivative. This yields the solution  $p_i(s) = [e^{-s\Gamma/m}]_{ii_0}$ , which corresponds to the initial condition  $p_i(0) = \delta_{i,i_0}$ . Next we consider  $P^{(n)}(s) := \langle p_{i_0}(s) \rangle_n |_{\varepsilon=0}$ , the mean return probability to the starting point after time  $s$ , where the average is taken over all critical percolation clusters with  $n$  sites. Clearly, these definitions are independent of the starting point  $i_0$ , because on average there is no distinguished site by assumption. Thus we can also write

$$P^{(n)}(s) = \left\langle \frac{1}{n} \text{Tr } e^{-s\Gamma/m} \right\rangle_n \Big|_{\varepsilon=0} \quad (53)$$

for finite  $n$ . The return probability behaves as [76, 95, 94]

$$P^{(n)}(s) \sim s^{-d_s/2} \mathcal{F}(s/s_n) + 1/n, \quad (54)$$

where  $s_n \sim n^{2/d_s}$  and the cut-off function  $\mathcal{F}(x)$  is of order one for  $x \lesssim 1$  and decreases rapidly to zero for  $x \rightarrow \infty$ . Basically, (54) says that for times  $s \gg s_n$  the walker has no memory of where he had started from. For times  $s \lesssim s_n$  the fractal-like nature of a cluster at  $c = c_{\text{crit}}$  leads to an algebraic decrease of the return probability, which involves the spectral dimension  $d_s$ . Now, assuming that  $\langle G(t) \rangle$  obeys the scaling form (37), the information provided by (54) for  $c = c_{\text{crit}}$  is sufficient to conclude [40] the exponent relations

$$\Delta = \frac{d_s}{2}(\tau - 1) \quad \text{and} \quad z = \frac{2}{d_s \sigma}. \quad (55)$$

When plugging (55) into (45), we recover (50) and get the new scaling relation

$$\ell = (1 - \tau + 4/d_s)/\sigma. \quad (56)$$

Since, the critical behaviour of Erdős–Rényi random graphs coincides with that of mean-field percolation, we get the missing exponents  $\Delta$  and  $z$  for that case by inserting the mean-field values into (55).

#### 4.2. Zimm dynamics

The matrix  $\tilde{\Gamma}$ , which determines stress relaxation, is by far more complicated than  $\Gamma$  in the presence of hydrodynamic interactions. In particular, it reflects cluster topology only in a much more subtle way than  $\Gamma$ . In fact, it was that apparent encoding of topology in  $\Gamma$  that made the analytical methods of the last subsection work. In the absence of suitable analytical tools, numerical methods remain to investigate stress relaxation in the Zimm model.

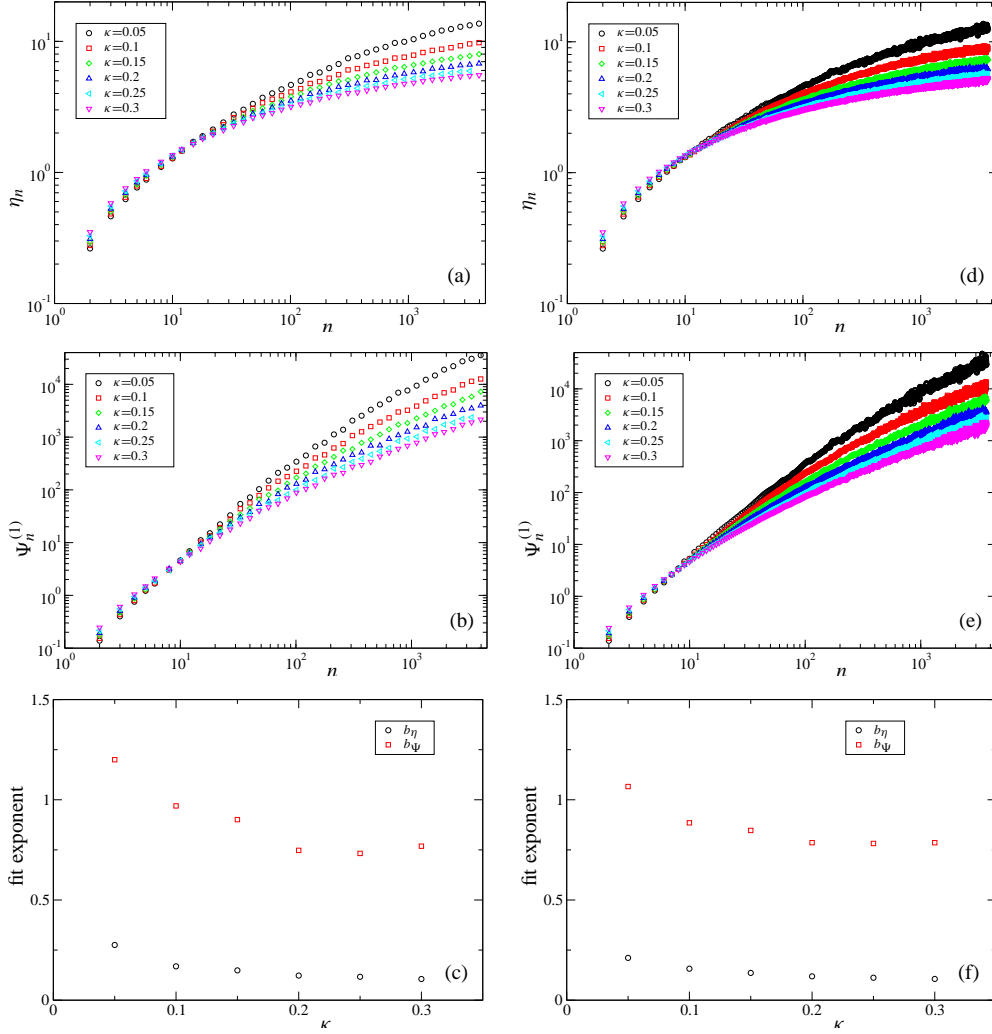


**Figure 3.** Numerical data to determine the scaling (57) for random clusters in the case of Erdős-Rényi random graphs (left column) and three-dimensional bond percolation (right column). In each case the averaged viscosity  $\eta_n$  (top) and normal stress coefficient  $\Psi_n^{(1)}$  (middle) are plotted for different strengths of the hydrodynamic interaction parameter  $\kappa$  as a function of the cluster size  $n$  on a double logarithmic scale. Power-law fits to the data yield the exponents  $b_\eta$  and  $b_\Psi$  as a function of  $\kappa$  (bottom).

We determined the scaling as  $n \rightarrow \infty$  of the partial averages

$$\eta_n := \langle \eta \rangle_n|_{\varepsilon=0} \sim n^{b_\eta} \quad \text{and} \quad \Psi_n^{(1)} := \langle \Psi^{(1)} \rangle_n|_{\varepsilon=0} \sim n^{b_\Psi} \quad (57)$$

at criticality by numerically diagonalising  $\tilde{\Gamma}$  and performing the disorder average over the crosslink ensemble [42]. The critical exponents  $k$  and  $\ell$  then follow from (25). All numerical computations were done with the Rotne-Prager-Yamakawa tensor for the hydrodynamic interactions. The reader who is interested in more details of the numerical computations is referred to [42].

In Figs. 3(a) and (b) we plot  $\eta_n$  and  $\Psi_n^{(1)}$  as a function of  $n$  on a double-logarithmic

scale for different values of the hydrodynamic interaction parameter  $\kappa$ . Crosslink statistics were chosen according to Erdős–Rényi random graphs. The exponents  $b_\eta$  and  $b_\Psi$  are obtained from power-law fits in the large  $n$ -range and are displayed in Fig. 3(c). The viscosity exponent decreases from  $b_\eta = 0.28$  for  $\kappa = 0.05$  to  $b_\eta = 0.11$  for  $\kappa = 0.3$ . We recall from (46) and (49) that the Rouse exponent for  $\kappa = 0$  is exactly given by  $b_\eta = 1/2$ . The exponent  $b_\Psi$  of the normal stress coefficient ranges from  $b_\Psi = 1.2$  for  $\kappa = 0.05$  to  $b_\Psi = 0.73$  for  $\kappa = 0.25$ . The exact Rouse value  $b_\Psi = (4/d_s) - 1 = 2$  for  $\kappa = 0$  follows from (48) and (25).

The same is done for three-dimensional bond percolation in the right column of Fig. 3. Figures 3(d) and (e) contain  $\eta_n$  and  $\Psi_n^{(1)}$ , respectively, as a function of  $n$  on a double-logarithmic scale for different values of  $\kappa$ . The exponents  $b_\eta$  and  $b_\Psi$ , extracted by fitting the curves in Figs. 3(d) and (e) to a power law for large  $n$ , are shown in Fig. 3(f). The numerical values for  $b_\eta$  are nearly identical to those obtained for Erdős–Rényi random graphs. Again, one observes a decrease from  $b_\eta = 0.21$  for  $\kappa = 0.05$  to  $b_\eta = 0.11$  for  $\kappa = 0.3$ . The exponent  $b_\Psi$  of the normal stress coefficient ranges from  $b_\Psi = 1.1$  for  $\kappa = 0.05$  to  $b_\Psi = 0.78$  for  $\kappa = 0.25$ . The corresponding exact Rouse values  $b_\eta = (2/d_s) - 1 \approx 1/2$  and  $b_\Psi = (4/d_s) - 1 \approx 2$  for  $\kappa = 0$  follow from (50) and (56) in the last subsection together with (25).

A careful analysis of the data in [42] reveals that the true Zimm exponents  $b_\eta$  and  $b_\Psi$  are universal in  $\kappa$  and that their seeming dependence on  $\kappa$  in Figs. 3(c) and (f) is most likely due to finite-size effects. More precisely, for small  $\kappa$  the data suffer from a crossover to their respective Rouse values so that they come out too large. For large  $\kappa$ , on the other hand, the asymptotics  $h(x) \sim 1 - (\pi x)^{-1/2}$  as  $x \rightarrow \infty$  of the lower line in (5) leads to a slower growth of  $b_\eta$  and  $b_\Psi$  at intermediate  $n$ . Hence, the exponents come out too small for larger  $\kappa$ . The most reliable values for the universal Zimm exponents  $b_\eta$  and  $b_\Psi$  should be obtained from around  $\kappa \approx 0.3$ . It is these values which are listed in Table 3 below. The critical behaviour of the averaged viscosity  $\langle \eta \rangle \sim \varepsilon^{-k}$  and of the averaged first normal stress coefficient  $\langle \Psi^{(1)} \rangle \sim \varepsilon^{-\ell}$  for a polydisperse gelling solution of crosslinked monomers then follows from (25). For the viscosity this implies a *finite* value at the gel point for both, Erdős–Rényi random graphs and three-dimensional bond percolation. In contrast, the first normal stress coefficient is found to diverge with an exponent that depends on the cluster statistics. Choosing the cluster statistics according to Erdős–Rényi random graphs, we find  $\ell \approx 0.54$ . The case of three-dimensional bond percolation leads to the higher value  $\ell \approx 1.3$ . These exponent values are less than a third in magnitude than the corresponding exact analytical predictions of the Rouse model from (56) with the corresponding cluster statistics. All exponent values are summarised in Table 3.

### 4.3. Discussion

A fairly complete scaling picture of the gelation transition has been obtained within Rouse dynamics. All critical exponents  $k$ ,  $\ell$ ,  $\Delta$  and  $z$  of the stress-relaxation function in the sol phase and at criticality could be expressed in terms of two independent static percolation exponents  $\sigma$  and  $\tau$  plus the spectral dimension  $d_s$  of the incipient percolating cluster, see the scaling relations (50), (55) and (56). These scaling relations and the resulting numerical exponent values listed in Table 3 contradict the predictions  $k = 2\nu - \beta$  and  $\Delta = d\nu/(d\nu + k)$  of earlier scaling arguments [80, 81, 84, 16, 87, 104]. What is the reason for this discrepancy? The scaling arguments involve the fractal Hausdorff dimension  $d_f := d - \beta/\nu$  of *rigid* percolation clusters at  $c_{\text{crit}}$ . Rouse clusters, however, are thermally stabilised, Gaussian phantom clusters with the fractal Hausdorff dimension  $d_f^{(G)}$ , see (27) [50, 52, 55]. The latter is different from  $d_f$  in space dimensions below the upper critical dimension  $d_u = 6$ . Indeed, if one replaces  $d_f$



**Table 3.** Summary of critical exponents for stress relaxation (see Eqs. (37), (44) and (57) for their definitions). The numerical values for Rouse dynamics are based on the scaling relations (49), (50), (55) and (56). Those for Zimm dynamics are based on the data analysis of Fig. 3. The values are listed for cluster statistics according to three-dimensional bond percolation (3D) and Erdős–Rényi random graphs (ER), and are compared to some experimental findings.

Exponent	Zimm		Rouse		[96]	[83]	[97]	[98]	[99]	[100]	[101]	[81]	[84]	[102]	[103]
	3D	ER	3D	ER											
$k$	(*)	(*)	0.71	0 <sup>(#)</sup>	0.2	0.7	0.82	1.1	1.27	1.3	1.36	1.4	>1.4	6.1	
$\ell$	1.3	0.54	4.1	3											
$\Delta$			0.79	1		0.72	0.71	0.69		0.67 – 0.68	0.66	0.70		0.33	0.69 – 0.77
$z$			3.3	3		2.9	2.67								
$b_\eta$	0.11	0.11	0.50	1/2											
$b_\Psi$	0.77	0.77	2.0	2											

(\*) no divergence

(#) logarithmic divergence

by  $d_f^{(G)}$  in these scaling arguments, as one should consistently do within a Rouse description, the results will coincide with the ones obtained here.

Since the long-standing scaling relations  $k = 2\nu - \beta$  and  $\Delta = d\nu/(d\nu + k)$  involve the Hausdorff fractal dimension  $d_f$  of rigid percolation clusters, it is sometimes argued that they describe the behaviour of a more realistic model, which, in addition to the interactions of the Rouse model, accounts for excluded-volume effects, too, see e.g. [104]. As far as we know, this claim has not been verified by analytical arguments within a microscopic model. One may even have doubts whether this claim is generally true: Extensive molecular-dynamics simulations [29] of a system of crosslinked soft spheres in three dimensions, with cluster statistics from percolation and an additional strongly repulsive interaction at short distances, yield the values  $k \approx 0.7$  and  $\Delta \approx 0.75$ , which are remarkably close to the predictions of the Rouse model for randomly crosslinked monomers, see Table 3. On the other hand, simulations of the bond-fluctuation model in [28] imply  $k \approx 1.3$  and are thus in favour of the claim. However, the viscosity is not measured directly in these latter simulations. Rather it is derived from the scaling of diffusion constants and an additional scaling assumption that may be questioned [29]. Hence, it is an open problem to what extent the critical Rouse exponents of Table 3 are modified by excluded-volume interactions.

In the context of dynamical critical phenomena, one usually expects dynamical scaling to hold. Thereby one can infer critical properties of the gel phase from those of the sol phase. In particular, the critical behaviour of the shear modulus  $G_0 \sim |\varepsilon|^\mu$  follows from the scaling form (37) of the stress-relaxation function. The result  $\mu = \Delta z = (\tau - 1)/\sigma$  involves only the two exponents  $\sigma$  and  $\tau$  of the cluster-size distribution. Using well-known scaling relations of percolation theory, this can be rewritten as  $\mu = d\nu$  in terms of the correlation-length exponent  $\nu$  and the spatial dimension  $d$ . It is in agreement with the simple scaling argument based on dimensional analysis of the free-energy density. In a recent letter [105], the scaling of entropic shear rigidity was analysed for both phantom chains and those with excluded-volume interactions. In both cases the gel was prepared by crosslinking a melt of chains with excluded-volume interactions. Our choice of percolation statistics combined with Rouse dynamics should be comparable to phantom chains prepared in an ensemble with excluded-volume interactions. However, the results of [105] for  $\mu$  disagree with the above dynamic-scaling argument. The reasons for the discrepancy are not understood.

Let us return to the sol phase and discuss the Zimm results, which are based on the exact numerical determination of the scaling exponents  $b_\eta$  and  $b_\Psi$  for the fixed-size averages

(57) of the viscosity and of the first normal stress coefficient. The resulting finiteness of the macroscopic viscosity  $\langle\eta\rangle$  at the transition is clearly the most serious drawback of the Zimm model for randomly crosslinked monomers. Also, this failure comes unexpected, because a well-known scaling argument [14, 106, 50] predicts a logarithmic divergence. This scaling argument uses the (correct) scaling  $D_n \sim 1/R_{\text{gyr},n}$  of diffusion constants together with the Stokes–Einstein relation and yields  $b_\eta = d/d_f - 1$ . Consequently, one gets from (25) the scaling relation  $k = (1 - \tau + d/d_f)/\sigma$ . Inserting hyperscaling and the fractal dimension of rigid percolation clusters, one would get  $k = 0$  from that, which was interpreted as a logarithmic divergence. But as we remarked already earlier on in this subsection, the correct fractal dimension  $d_f$  for Gaussian phantom clusters is  $d_f^{(\text{G})}$ . For both cluster statistics this would give an unphysical negative value around  $-1/4$  for  $b_\eta$  which can be definitely ruled out by our data.<sup>§</sup> Thus, we conclude that the scaling approach of [14, 106, 50] does not apply to the Zimm model for randomly crosslinked monomers. Another scaling approach to this model by [17] is also falsified by our data. On the other hand, Brownian-dynamics simulations of hyperbranched polymers were performed in [91]. They also account for *fluctuating* hydrodynamic interactions corresponding to  $\kappa = 0.35$ , as well as for excluded-volume interactions and lead to  $b_\eta = 0.13$ . This result is remarkably close to our finding  $b_\eta \approx 0.11$  for the highest coupling strength  $\kappa = 0.3$  that we have considered, whereas experimental findings (see below) are consistently above our value.

Next, we comment on how the Rouse and Zimm predictions for stress relaxation compare to experimental reality. Table 3 shows an enormous scatter of the experimental data. Thus, a serious check of theoretical predictions is currently severely hampered. The origin of this wide spread of the data is unclear so that even the question arose, whether the dynamical critical behaviour at the gelation transition was indeed universal [107]. Possible explanations for non-universal behaviour include the splitting of a static universality class into two dynamical ones [92, 17] and, for the case of crosslinking long polymer-chain molecules (vulcanisation), a decrease of the width of the critical region with increasing chain length [108]. The latter may explain the observation of a crossover behaviour to mean-field properties in certain gelation experiments, if measurements were not performed well inside the true critical region.

As far as we know, no measurements of the critical behaviour of the first normal stress coefficient have been reported. The Rouse value  $k \approx 0.71$  for the viscosity and three-dimensional percolation statistics agrees well with the experiments of [79, 107, 80, 83] (only [83] was included in Table 3 to demonstrate the broad scatter of the viscosity data). On the other hand, it is not compatible with the possibly oversimplifying albeit attractive proposal [92, 17] to interpret the wide variation of the viscosity exponent  $k$  as a signature of a splitting of the static universality class of gelation into different dynamic ones. Indeed, Rouse and Zimm dynamics are considered [109, 48] to be at the extreme ends of the strength of the hydrodynamic interaction. Since the Zimm model does not even predict a divergence at the transition, the actual value of  $k$  should then lie below the Rouse value according to that proposal.

Hence, the broad scatter of the experimental data calls for additional relevant interactions beyond those accounted for in the Zimm or Rouse model. This may be due to the preaveraging approximation. In particular, it throws away hydrodynamic interactions among different clusters. But we do not expect this to be the sole relevant simplification of the Zimm model, because linear polymers show a decrease in the viscosity when abandoning the preaveraging approximation [110], and effects of preaveraging for branched molecules are even more

<sup>§</sup> Unfortunately, the value of  $b_\eta$  resulting from this scaling argument in the case of Erdős–Rényi random graphs was incorrectly ascribed to  $d = 6$  dimensions in the second last paragraph of [42], leading to the wrong statement  $b_\eta = 1/2$  there.

pronounced than those for linear ones [111]. Rather it seems that there are no satisfactory explanations without considering excluded-volume interactions. Indeed, simulations [28] of the bond-fluctuation model deliver higher values  $k \approx 1.3$  in accordance with the scaling relation  $k = 2\nu - \beta$ , which arises from heuristically merging Rouse-type and excluded-volume properties, see above. On the other hand, entanglement effects are neglected, too. These topological interactions are argued to play a vital role in stress relaxation. However, *temporary* entanglements are expected to play only a minor role [84] for the dynamics close to the gelation transition. This is because the time scale of a temporary entanglement is determined by the smaller clusters, whereas near-critical dynamics is determined by the largest clusters, which contribute the longest time scales. Yet, there remain *permanent* entanglements due to interlocking loops. They are clearly far beyond the scope of the present and many other theoretical approaches.

## 5. Closing remarks

The list of shortcomings of the Rouse and the Zimm model for crosslinked monomers is long, and it was discussed in Sections 3.3 and 4.3. Yet, one should not underestimate the importance of these models for our understanding of gelling liquids. First, the success of Theoretical Physics and, in particular, Statistical Physics has always relied on capturing the essence of observable phenomena in simple mathematical models. Models that isolate certain physical mechanisms and, at the same time, sacrifice many details of the observed reality. It is safe to say that, at least for linear polymers, the Rouse and the Zimm model have proven to be among this class [47, 48]. Second, simple exactly solvable models always represent cornerstones against which more elaborate theories, approximation methods and numerical simulations can be tested. Moreover, in the absence of an ultimate theoretical picture, the predictions of such minimal models also serve as a standard reference for experimental data. Indeed, this has been common practice in experimental investigations on gelling liquids over the years, see e.g. the review articles [112, 44]. All the more it is important to have reliable and mathematically firmly based predictions of these model.

## Acknowledgments

We gratefully acknowledge the collaboration with M. Küntzel on self-diffusion in the Zimm model. This work was supported by the Deutsche Forschungsgemeinschaft (DFG) under grant numbers Zi 209/6-1, Zi 209/7-1, Mu 1056/2-1 and through SFB 602.

## References

- [1] Flory P J 1992 *Principles of polymer chemistry* 15th printing (Ithaca: Cornell University Press)
- [2] Larson R G 1999 *The structure and rheology of complex fluids* (New York: Oxford University Press)
- [3] Carothers W H 1936 *Trans. Faraday Soc.* **32** 39
- [4] Flory P J 1941 *J. Am. Chem. Soc.* **63** 3083, 3091, 3096
- [5] Flory P J 1942 *J. Phys. Chem.* **46** 132
- [6] Stockmayer W H 1943 *J. Chem. Phys.* **11** 45
- [7] Stockmayer W H 1944 *J. Chem. Phys.* **12** 125
- [8] Fisher M E and Essam J W 1961 *J. Math. Phys.* **2** 609
- [9] Stephen M J 1977 *Phys. Rev. B* **15** 5674
- [10] Stauffer D and Aharony A 1994 *Introduction to percolation theory* revised 2nd ed (London: Taylor and Francis)
- [11] Stauffer D 1976 *J. Chem. Soc. Faraday Trans. II* **72** 1354
- [12] de Gennes P-G 1976 *La Recherche* **7** 919

- [13] Plischke M and Bergersen B 1994 *Equilibrium statistical physics* 2nd ed (Singapore: World Scientific)
- [14] Stauffer D, Coniglio A and Adam M 1982 *Adv. Polym. Sci.* **44** 103
- [15] de Gennes P-G 1993 *Scaling concepts in polymer physics* 4th printing (Ithaca: Cornell University Press)
- [16] de Gennes P-G 1978 *Comptes Rendus Acad. Sci. (Paris)* **286B** 131
- [17] Arbabi S and Sahimi M 1990 *Phys. Rev. Lett.* **65** 725
- [18] Sahimi M 1994 *Applications of percolation theory* (London: Taylor and Francis)
- [19] Goldbart P M, Castillo H E and Zippelius A 393 *Adv. Phys.* **45** 1996
- [20] Zippelius A and Goldbart P M 1997 *Spin glasses and random fields* ed A P Young (Singapore: World Scientific) pp 357
- [21] Theissen O, Zippelius A and Goldbart P M 1945 *Int. J. Mod. Phys. B* **11** 1997
- [22] Castillo H E and Goldbart P M R24 *Phys. Rev. E* **58** 1998
- [23] Peng W, Castillo H E, Goldbart P M and Zippelius A 839 *Phys. Rev. B* **57** 1998
- [24] Castillo H E, Goldbart P M and Zippelius A 14702 *Phys. Rev. B* **60** 1999
- [25] Peng W and Goldbart P M 3339 *Phys. Rev. E* **61** 2000
- [26] Broderix K, Weigt M and Zippelius A 2002 *Eur. Phys. J. B* **29** 441
- [27] Mukhopadhyay S, Goldbart P M and Zippelius A 2004 *Europhys. Lett.* **67** 49
- [28] Del Gado E, de Arcangelis L and Coniglio A 2000 *Eur. Phys. J. E* **2** 359
- [29] Vernon D, Plischke M and Joós B 2001 *Phys. Rev. E* **64** 031505
- [30] Jespersen S N 2002 *Phys. Rev. E* **66** 031502
- [31] Del Gado E, de Arcangelis L, Coniglio A 2002 *Phys. Rev. E* **65** 041803
- [32] Plischke M, Vernon D C, Joós B 2003 *Phys. Rev. E* **67** 011401
- [33] Jespersen S N, Plischke M 2003 *Phys. Rev. E* **68** 021403
- [34] Del Gado E, Fierro A, de Arcangelis L and Coniglio A 2004 *Phys. Rev. E* **69** 051103
- [35] Broderix K, Goldbart P M and Zippelius A 1997 *Phys. Rev. Lett.* **79** 3688
- [36] Broderix K, Löwe H, Müller P and Zippelius A 1999 *Europhys. Lett.* **48** 421
- [37] Broderix K, Löwe H, Müller P and Zippelius A 2001 *Phys. Rev. E* **63** 011510
- [38] Broderix K, Löwe H, Müller P and Zippelius A 2001 *Physica A* **302** 279
- [39] Broderix K, Müller P and Zippelius A 2002 *Phys. Rev. E* **65** 041505
- [40] Müller P 2003 *J. Phys. A* **36** 10443
- [41] Küntzel M, Löwe H, Müller P and Zippelius A 2003 *Eur. Phys. J. E* **12** 325
- [42] Löwe H, Müller P and Zippelius A 2004 *J. Chem. Phys.* in press
- [43] Martin J E and Wilcoxon J P 1988 *Phys. Rev. Lett.* **61** 373
- [44] Winter H H and Mours M 1997 *Adv. Polym. Sci.* **134** 165
- [45] Rouse P E 1953 *J. Chem. Phys.* **21** 1272
- [46] Zimm B H 1956 *J. Chem. Phys.* **24** 269
- [47] Bird R B, Curtiss C F, Armstrong R C and Hassager O 1987 *Dynamics of polymeric liquids* vol 2, 2nd ed (New York: Wiley)
- [48] Doi M and Edwards S F 1988 *The theory of polymer dynamics* (Oxford: Clarendon Press)
- [49] Eichinger B E 1980 *Macromolecules* **13** 1
- [50] Cates M E 1984 *Phys. Rev. Lett.* **53** 926
- [51] Cates M E 1985 *J. Physique (France)* **46** 1059
- [52] Neuburger N A and Eichinger B E 1985 *J. Chem. Phys.* **83** 884
- [53] Vilgis T A 1988 *Physica A* **153** 341
- [54] Shy L Y and Eichinger B E 1989 *J. Chem. Phys.* **90** 5179
- [55] Sommer J-U, Schulz M and Trautenberg H L 1993 *J. Chem. Phys.* **98** 7515
- [56] Sommer J-U and Blumen A 1995 *J. Phys. A: Math. Gen.* **28** 6669
- [57] Zimm B H and Kilb R W 1996 *J. Pol. Sci., Part B, Polymer Physics Ed.* **34** 1367
- [58] Blumen A and Jurjiu A 2002 *J. Chem. Phys.* **116** 2636
- [59] von Ferber C and Blumen A 2002 *J. Chem. Phys.* **116** 8616
- [60] Jurjiu A, Koslowski T and Blumen A 2003 *J. Chem. Phys.* **118** 2398
- [61] Kirkwood J G and Riseman J 1948 *J. Chem. Phys.* **16** 565
- [62] Oseen C W 1910 *Ark. Mat. Astr. Fys.* **6** (29) 1
- [63] Rotne J and Prager S 1969 *J. Chem. Phys.* **50** 4831
- [64] Yamakawa H 1970 *J. Chem. Phys.* **53** 436
- [65] Fixman M 1983 *J. Chem. Phys.* **78** 1594
- [66] Albert A E 1972 *Regression and the Moore–Penrose pseudoinverse* (New York: Academic Press)
- [67] Klein D J and Randić M 1993 *J. Math. Chem* **12** 81
- [68] Erdős P and Rényi A 1960 *Publ. Math. Inst. Hung. Acad. Sci. A* **5** 17; reprinted in: Spencer J (ed) 1973 *P. Erdős: the art of counting* (Cambridge, MA: MIT Press) Chap 14, Article 324
- [69] Martin J E, Wilcoxon J and Odinek J 1991 *Phys. Rev. A* **43** 858
- [70] de Gennes P-G 1979 *J. Physique (France) Lett.* **40**, L-197

- [70] Öttinger H C 1987 *J. Chem. Phys.* **87** 3156
- [71] Simon B 1979 *Functional integration and quantum physics* (New York: Academic Press)
- [72] Meir A and Moon J W 1970 *J. Combinatorial Theory* **8** 99
- [73] Harris A B and Lubensky T C 1987 *Phys. Rev. B* **35** 6964
- [74] Stenull O, Janssen H K and Oerding K 1999 *Phys. Rev. E* **59** 4919
- [75] Nakayama T, Yakubo K and Orbach R L 1994 *Rev. Mod. Phys.* **66** 381
- [76] Bunde A and Havlin S 1996 *Fractals and disordered systems* ed A Bunde and S Havlin (Berlin: Springer) pp 59, 115
- [77] Adam M, Delsanti M, Munch J P and Durand D 1988 *Phys. Rev. Lett.* **61** 706
- [78] Bauer J and Burchard W 1992 *J. Phys. II (France)* **2** 1053
- [79] Adam M, Delsanti M, Durand D, Hild G and Munch J P 1981 *Pure Appl. Chem.* **53** 1489
- [80] Durand D, Delsanti M, Adam M and Luck J M 1987 *Europhys. Lett.* **3** 297
- [81] Martin J E, Adolf D and Wilcoxon J P 1988 *Phys. Rev. Lett.* **61** 2620
- [82] Adolf D and Martin J E 1990 *Macromolecules* **23** 3700
- [83] Devreux F, Boilot J P, Chaput F, Malier L and Axelos M A V 1993 *Phys. Rev. E* **47** 2689
- [84] Colby R H, Gillmor J R and Rubinstein M 1993 *Phys. Rev. E* **48** 3712
- [85] Vlassopoulos D, Chira I, Loppinet B and McGrail P T 1998 *Rheol. Acta* **37** 614
- [86] Tordjeman P, Fargette C and Mutin P H 2001 *J. Rheol.* **45** 995
- [87] Martin J E, Adolf D and Wilcoxon J P 1989 *Phys. Rev. A* **39** 1325
- [88] Rubinstein M, Zurek S, McLeish T C B and Ball R C 1990 *J. Physique (France)* **51** 757
- [89] Zilman A G and Granek R 1998 *Phys. Rev. E* **58** R2725
- [90] Broderix K, Aspelmeier T, Hartmann A K and Zippelius A 2001 *Phys. Rev. E* **64** 021404
- [91] Sheridan P F, Adolf D B, Lyulin A V, Neelov I and Davies G R 2002 *J. Chem. Phys.* **117** 7802
- [92] Daoud M and Lapp A 1990 *J. Phys. Cond. Matter* **2** 4021
- [93] Merris R 1994 *Linear Algebra Appl.* **197–198** 143
- [94] Alexander S and Orbach R 1982 *J. Physique (France)* **43** L-625
- [95] Havlin S and Ben-Avraham D 2002 *Adv. Phys.* **51** 187
- [96] Takigawa T, Urayama K and Masuda T 1990 *J. Chem. Phys.* **93** 7310
- [97] Axelos M A V and Kolb M 1990 *Phys. Rev. Lett.* **64** 1457
- [98] Adam M, Lairez D, Karpasas M and Gottlieb M 1997 *Macromolecules* **30** 5920
- [99] Zheng H, Zhang Q, Jiang K, Zhang H and Wang J 1996 *J. Chem. Phys.* **105** 7746
- [100] Takahashi M, Yokoyama K, Masuda T 1994 *J. Chem. Phys.* **101** 798
- [101] Lusignan C P, Mourey T H, Wilson J C and Colby R H 1995 *Phys. Rev. E* **52** 6271
- [102] Lusignan C P, Mourey T H, Wilson J C and Colby R H 1999 *Phys. Rev. E* **60** 5657
- [103] Tixier T, Tordjeman P, Cohen-Solal G and Mutin P H 2004 *J. Rheol.* **48** 39
- [104] Rubinstein M, Colby R H and Gillmor J R 1989 *Space-time organization in macromolecular fluids* ed F Tanaka, M Doi and T Ohta (New York: Springer)
- [105] Xiangjun Xing, Mukhopadhyay S and Goldbart P M 2004 *Phys. Rev. Lett.* **93** 225701
- [106] Muthukumar M 1985 *J. Chem. Phys.* **83** 3161
- [107] Adam M, Delsanti M and Durand D 1985 *Macromolecules* **18** 2285
- [108] de Gennes P-G 1977 *J. Physique (Paris)* **38** L-355
- [109] Oono Y 1985 *Adv. chem. Phys.* **61** 301
- [110] Fixman M 1981 *Macromolecules* **14** 1710
- [111] Burchard W, Schmidt M and Stockmayer W H 1980 *Macromolecules* **13** 580
- [112] Martin J E and Adolf D 1991 *Annu. Rev. Phys. Chem.* **42** 311